Available online at www.sciencedirect.com

SCIENCE DIRECT®

Journal of Fluorine Chemistry 123 (2003) 119–126

JOURNAL OF FLUORINE CHEMISTRY

www.elsevier.com/locate/jfluchem

Coupling between a fluorinated olefin and a perfluorinated iodide: a model study on the reaction mechanism of perfluorinated polymer cross-linking

I. Wlassics*, E. Barchiesi, M. Sala

Solvay Solexis, Via S. Pietro, 50-20021 Bollate (MI), Italy

Received 17 July 2002; received in revised form 31 March 2003; accepted 2 April 2003

Abstract

In a model study, ^{1}H, ^{19}C, ^{13}C-^{1}H and ^{1}H-^{1}H correlated NMR techniques confirm a Markovnikov type reaction intermediate for the major coupling products between a short, low MW perfluorinated iodide C_2F_5I (**I**) and a short, low MW fluorinated olefin $CF_3(CF_2)_7CH{=}CH_2$ (**II**). The reaction is peroxide induced (di-*t*-butyl peroxide, DTBP) and is conducted at 140 °C for a 3 h reaction time in a sealed glass ampoule. Side reaction products due to the reaction of DTBP with radical reaction intermediates were also observed and identified. The study aimed to mimic as closely as possible the peroxide-initiated coupling reaction between an iodine terminated fluoropolymer (model compound **I**) and its fluorinated di-olefin coupling agent (model compound **II**). A mono-olefin was chosen to simplify the model reaction.

Keywords: Polymer; Peroxide; Coupling; Model study

1. Introduction

Peroxide-initiated coupling between an iodine terminated fluoropolymer and a fluorinated di-olefin gives improved thermal resistance to the resulting fluoropolymer [1,2] with respect to the consolidated classical ionic [3] or radical coupling mechanisms [4,5]. Previous model studies of the coupling of elastomers performed by Logothetis [5], Apotheker et al. [6], Krusic and Kochi [7] and Meakin and Krusic [8], employing brominated substrates and a peroxide [9,10] have unequivocally demonstrated, with the aid of ESR, that the mechanism of peroxide curing of fluoroelastomers is a radical process. Furthermore, it was demonstrated that the most thermally stable cross-links were obtained when triallyl isocyanurate (TAIC) was employed as the coupling agent [6]. A reaction mechanism was proposed [5,6] showing in part the fate of the radicals produced during the initiation and propagation steps.

The main intermediates and the reaction side products were not isolated or identified. The fate of the halogen atoms on the polymeric chain, in the course of the coupling reaction, proves to be of vital importance in the elucidation of a radically induced reaction mechanism.

This model study aimed to synthesize, isolate and/or identify, all of the reaction products generated in a radically induced coupling reaction. As a result of this model study we hope to have made progress in both confirming and completing the hypothesis of Apotheker and others [5–7].

2. Results and discussion

2.1. Model coupling reaction mechanism

A careful analysis of ^{1}H, ^{19}F, correlated ^{1}H-^{13}C NMR and COSY ^{1}H-^{1}H NMR spectra of the reaction mixture, purified of its starting materials **I** and **II** as well as of di-*t*-butyl peroxide (DTBP) and its decomposition by-products acetone and *t*-butanol [11–14], reveals that the major event in the model study is the Markovnikov addition of the perfluorinated radical $CF_3CF_2^{\bullet}$ to the terminal vinyl carbon of **II**, $C_8F_{19}CH{=}\underline{C}H_2$, thereby generating the more stable secondary radical at the C-9 position of **III** as shown in Fig. 1. The other mechanism possible would be the anti-Markovnikov addition of the $C_2H_5^{\bullet}$ radical to the C-9 position of compound **II** generating the less stable primary radical at the

---

[*] Corresponding author. Tel.: +39-02-38356367; fax: +39-02-38356355.
E-mail address: ivan.wlassics@solvay.com (I. Wlassics).

0022-1139/$ – see front matter © 2003 Elsevier B.V. All rights reserved.
doi:10.1016/S0022-1139(03)00110-6

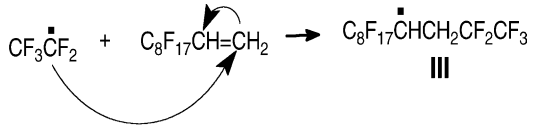

Fig. 1. Markovnikov reaction pathway leading to the radical intermediate **III**.

C-10 position of compound **III**. This is in accord with the studies by Tarrant and Tandon [15].

Olefin **II** is known to show moderate to good reactivity under radical conditions [16–18] and in coupling reactions, as shown by Arcella et al. [19].

Fig. 1 shows the expected mode of attack and follows Markovnikov's rule due mainly to the formation of the more stable radical as postulated by Tedder and Walton [20]. The existence of intermediate **III** depicted in Fig. 1 is demonstrated by the ^{1}H, ^{19}F, ^{1}H-^{1}H COSY and ^{1}H-^{13}C correlated NMR spectra shown respectively in Figs. 2–5. The NMR spectra unequivocally assign the frequencies typical of the secondary iodides **IV** and **V** shown respectively in Figs. 6 and 7. The secondary iodides **IV** and **V** can in fact only arise from intermediate **III**. The NMR assignments are in accord with those reported by Jeanneaux et al., Wiberg et al., Tonelli et al. [21a,b,c] for similar compounds.

The discrimination between the Markovnikov product **IV** shown in Fig. 6 and the anti-Markovnikov product **VI** shown in Fig. 8 is demonstrated in the ^{1}H-^{13}C heteronuclear single quantum correlation with gradient selection (g-HSQC) NMR spectrum shown in Fig. 3. In fact, if compound **VI** were present, we would expect a chemical shift of 0 ppm for the primary iodide $-CF_2-\underline{CH_2}-I$ [21b,c] which was absent. Furthermore, from both the shift and the multiplicity analysis of the peak at 5.2 ppm observed in Fig. 3 (doublet of triplets, $^1J(^{13}C, ^1H) = 152$ Hz and $^2J(^{13}C, ^{19}F) = 26$ Hz, coupling constant spectral data not shown), typical of the secondary iodide moiety $-\underline{CH}(I)-CF_2-$ [21b,c], one can unequivocally assign the NMR spectrum shown in Fig. 3, and consequently in Figs. 2, 4 and 5, to the Markovnikov compounds **IV** and **V**.

The observation of the absence of the anti-Markovnikov product **VI** confirms both the stability of the intermediate radical **III** [20] and the hypothesis that the secondary radical species **III** is the only major intermediate in the model coupling reaction.

As was to be expected, multiple coupling events typical of a radical coupling mechanism were observed. The principal multiply coupled product observed arises from the coupling of radical **III** formed as shown in Fig. 1 to the olefin **II**.

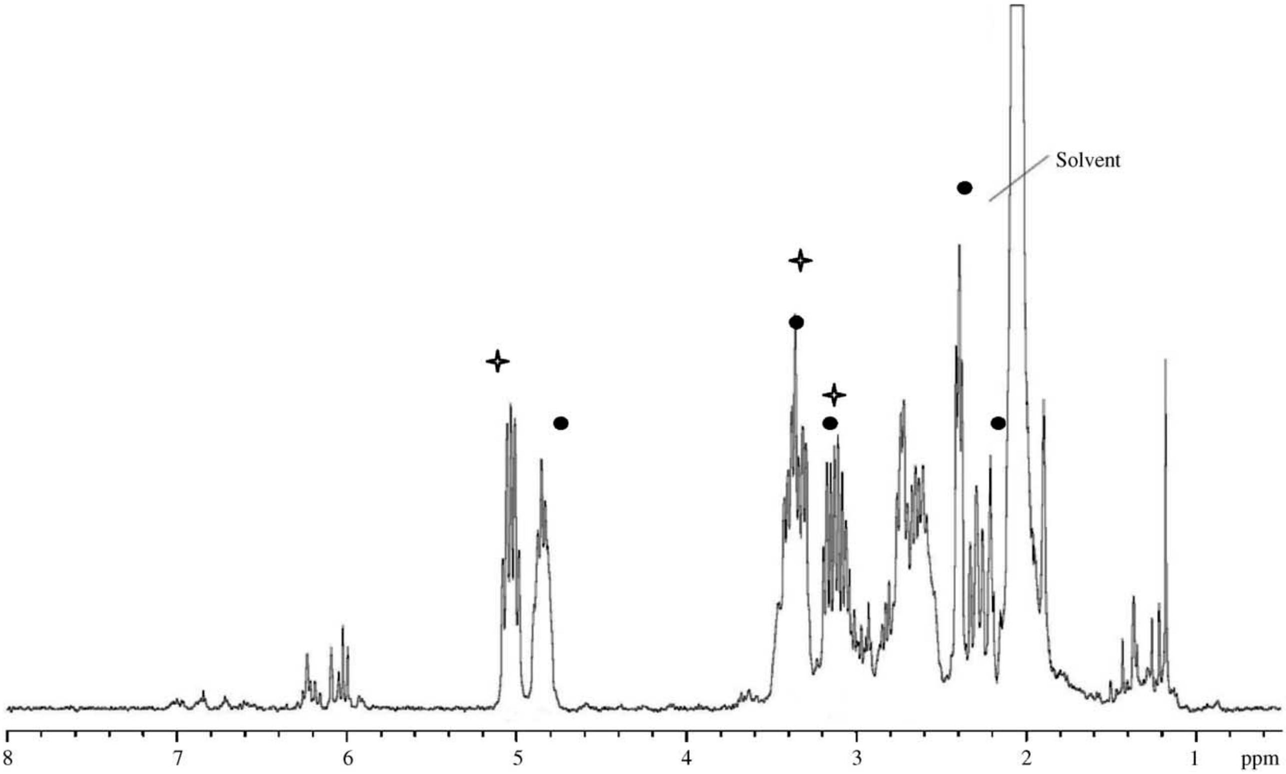

Fig. 2. ^{1}H NMR spectrum of the isolated coupled products **IV** and **V**. The callouts correspond to the underlined portions of each structure:

✦ $CF_3CF_2\underline{CH_2CH(I)}CF_2CF_2(CF_2)_4CF_2CF_3$ **(IV)**

● 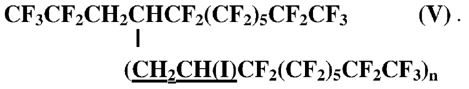

$$\begin{array}{l} CF_3CF_2CH_2CHCF_2(CF_2)_5CF_2CF_3 \qquad (V). \\ \qquad\qquad\quad | \\ \qquad\quad (\underline{CH_2CH(I)}CF_2(CF_2)_5CF_2CF_3)_n \end{array}$$

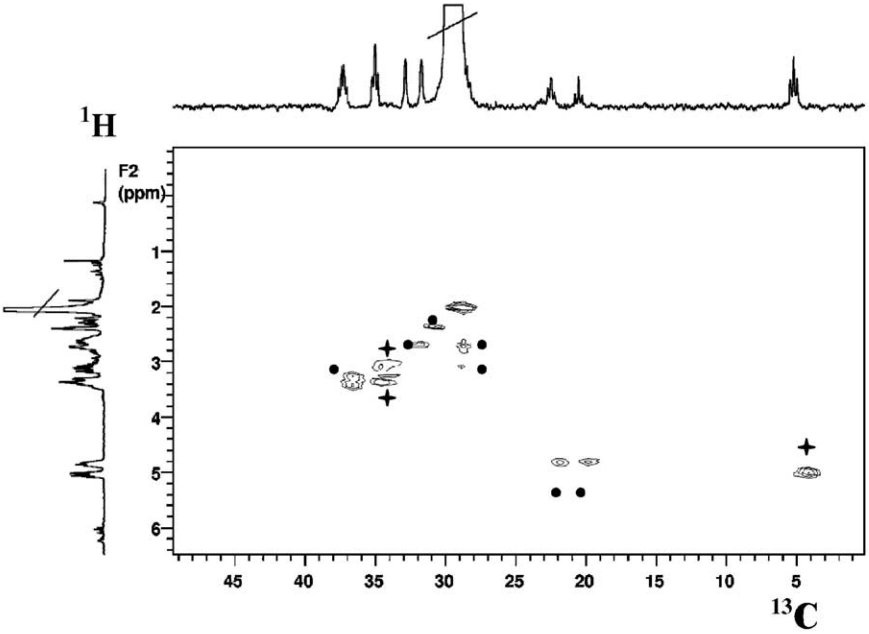

Fig. 3. ^{1}H-^{13}C heteronuclear single quantum correlation with gradient selection (g-HSQC) NMR spectrum of the isolated coupled products **IV** (+) and **V** (●). The callouts correspond to the underlined portions of each structure as in Fig. 2.

This coupling reaction again follows Markovnikov's rule [20] and a secondary iodide **V** with $n = 1$ is the product generated as shown in Fig. 7. Due to our experimental conditions, we only observed **V** with $n = 1$. It is likely that, operating in a large excess of **II**, and employing a larger quantity of fluorinated solvent (see Section 4.4), thereby making the reaction mixture less viscous, one could perhaps observe **V** with $n > 1$. The generation of $CF_3CF_2^{\bullet}$ is shown

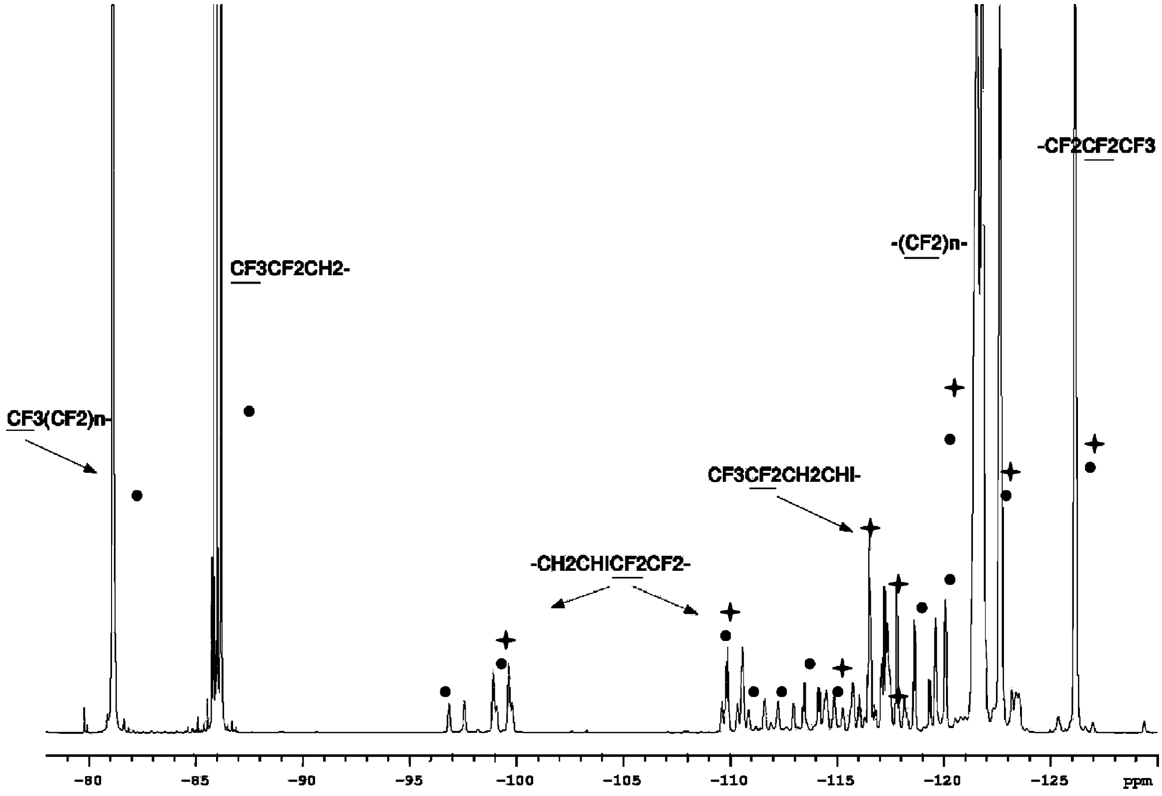

Fig. 4. ^{19}F NMR spectrum of the isolated coupled products **IV** (+) and **V** (●).

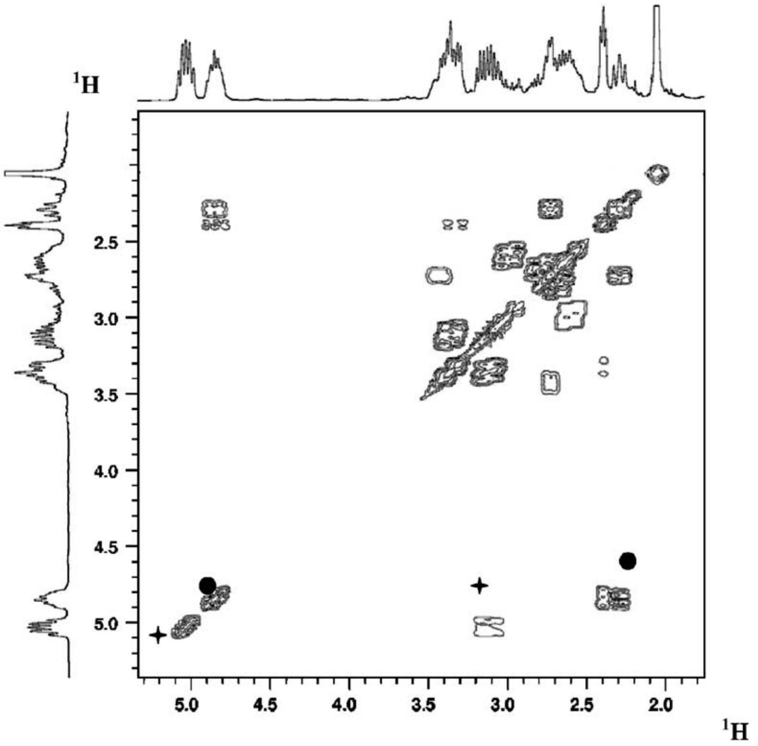

Fig. 5. ^1H-^1H g-COSY correlated NMR spectrum of the coupled products **IV** (+) and **V** (●). The callouts correspond to the underlined portions of each structure as in Fig. 2.

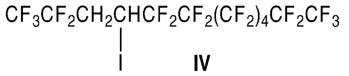

$CF_3CF_2CH_2\underset{\overset{|}{I}}{CH}CF_2CF_2(CF_2)_4CF_2CF_3$

IV

Fig. 6. Isolated model coupled Markovnikov product **IV**.

further on in the propagation step of Fig. 9. The reactions leading to products **IV** and **V** shown respectively in Figs. 9 and 10, can be viewed as a simplified version of the "pseudo-living polymerization" ([22–24] and references therein).

The formation of the observed major product **IV** most likely follows the generally accepted initiation–propagation steps [25,26] shown in Fig. 9. Fig. 9 shows all of the steps that occur which can explain the observed products but does not take into consideration all of the theoretically possible reactions. During the formation of **IV**, two propagation sequences are proposed involving intermediate **III**, propagation b and c. Although propagation sequence c may occur, the most probable route to **IV** is propagation sequence b, since the concentration of **I** is much higher than that of CH_3I (which arises from the decomposition of DTBP). The same reasoning can be applied to the scheme shown in Fig. 10; although propagation sequences c, d and e may all occur, the most probable route to **V** is propagation sequence c since the concentration of C_2H_5I is higher than the concentration of the methyl radical $CH_3^{\bullet}$ and the coupled product **IV** is bulkier and therefore less mobile and is always at a lower concentration than **I**.

It was observed that the selectivity of formation of product **IV** with respect to product **V** was 60:40, respectively (see Section 4.4). This, according to Apostolo et al. [22] and Arcella and Apostolo [24], was expected; as the molecular weight of the growing radical increases, its mobility

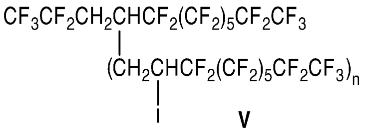

$CF_3CF_2CH_2\underset{(CH_2\underset{\overset{|}{I}}{CH}CF_2(CF_2)_5CF_2CF_3)_n}{\underset{|}{CH}}CF_2(CF_2)_5CF_2CF_3$

V

Fig. 7. Isolated model multiply coupled Markovnikov product **V**.

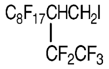

$C_8F_{17}\underset{\underset{CF_2CF_3}{|}}{CH}CH_2I$

VI

Fig. 8. Anti-Markovnikov product **VI**.

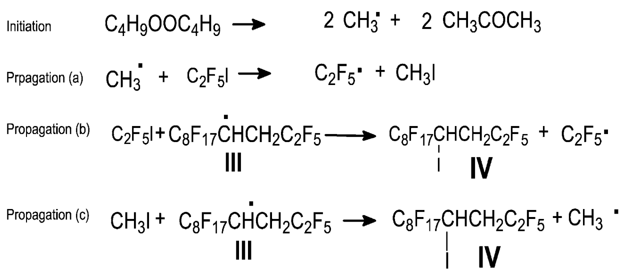

Initiation $C_4H_9OOC_4H_9 \rightarrow 2\,CH_3^{\bullet} + 2\,CH_3COCH_3$

Prpagation (a) $CH_3^{\bullet} + C_2F_5I \rightarrow C_2F_5^{\bullet} + CH_3I$

Propagation (b) $C_2F_5I + C_8F_{17}\underset{\mathbf{III}}{\dot{C}H}CH_2C_2F_5 \longrightarrow C_8F_{17}\underset{\overset{|}{I}}{CH}CH_2C_2F_5 + C_2F_5^{\bullet}$ **IV**

Propagation (c) $CH_3I + C_8F_{17}\underset{\mathbf{III}}{\dot{C}H}CH_2C_2F_5 \rightarrow C_8F_{17}\underset{\overset{|}{I}}{CH}CH_2C_2F_5 + CH_3^{\bullet}$ **IV**

Fig. 9. Reaction pathway leading to the Markovnikov radical intermediate **III** and the model coupled product **IV**.

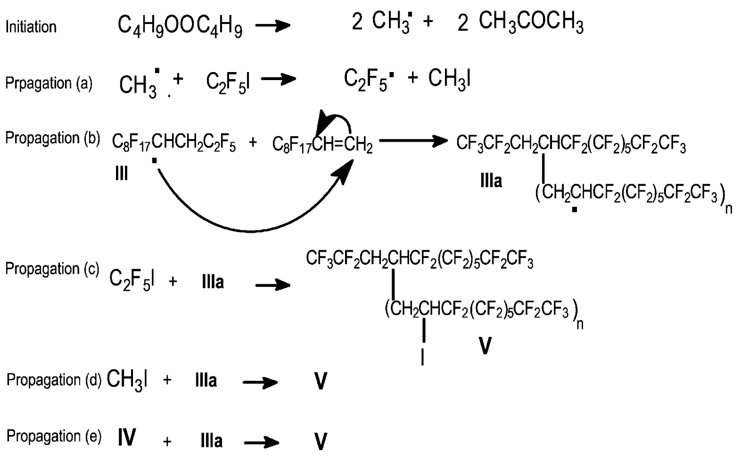

Fig. 10. Reaction pathway leading to the Markovnikov radical intermediate **IIIa** and the model multiply coupled product **V**.

decreases. The result is an almost exponential decrease in yield of the multiply coupled products. This is the principle of molecular weight polydispersity observed in polymer chemistry. Our simple model therefore, fits well with the reported literature [22–24].

Careful GC–MS analysis of the worked-up reaction mixture, shown in Fig. 11, confirmed the existence respectively of the coupled and multiply coupled products **IV** and **V**.

The total isolated yield of the coupled products **IV** and **V** was calculated to be 42 ± 2% (mol%) based on the isolated weight and on the ^{1}H NMR spectrum.

The peaks appearing in the NMR spectrum shown in Fig. 2 not pertaining to compound **IV** and **V** are attributed to (a) residual starting compound **II** (–CH=CH$_2$ resonance at 6.05 and 6.2 ppm); (b) residual *t*-butanol (–(CH$_3$)$_3$ at 1.1 ppm); (c) residual ether 2 (–(CH$_3$)$_3$ at 1.3 ppm).

Fig. 12 schematically shows the complete coupling reaction pathway along with all of the possible reaction products. The products shown in bold and in italics were the ones actually observed and identified.

2.2. *Coupling reaction side products*

As can be seen from Fig. 12, along with the two major coupling products **IV** (single coupling) and **V** (multiple coupling) isolated and identified, three side products were identified (but not isolated): (1) $CF_3CF_2CH_2COCH_3$, (2) $CF_3CF_2OC(CH_3)_3$, (3) CH_3I. All three side products were identified by ^{1}H NMR spectroscopy in the crude reaction mixture after complete removal of any residual acetone and *t*-butanol by repeated extractions of the crude mixture with distilled H$_2$O.

The total yield of the identified side products was calculated to be approximately 4 ± 0.2% (mol%) with respect to the limiting reagent (**II**) based on ^{1}H NMR spectroscopic analysis of the crude reaction mixture.

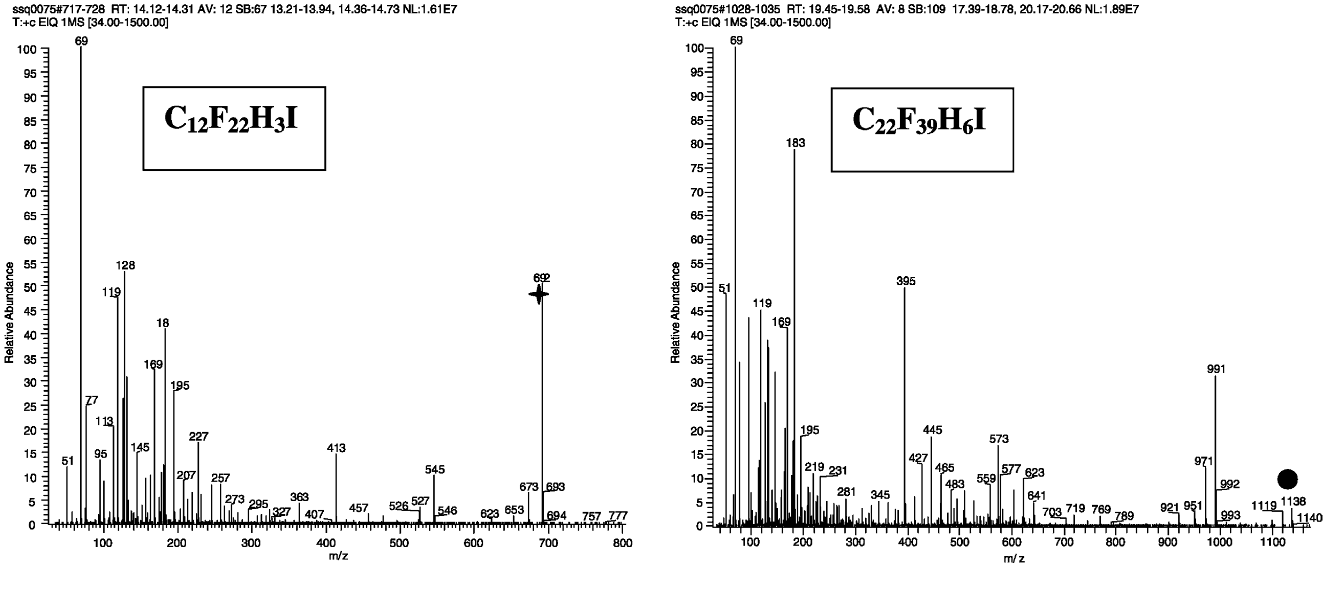

Fig. 11. GC–MS spectra of coupled products **IV** (✚, $C_{12}F_{22}H_3I$) and **V** (●, $C_{22}F_{39}H_6I$).

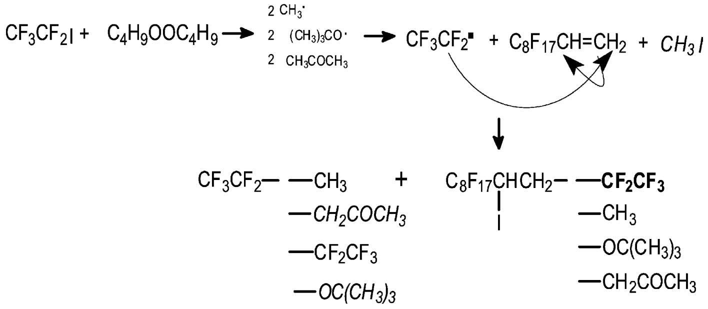

Fig. 12. Model of radical coupling showing the reaction mechanism, the coupled products obtained (bold) and the major side products observed (italics).

Aside from methyl iodide, whose presence is of no surprise if DTBP is employed as a radical initiator in the presence of an iodide [14,27,28], compounds 1 and 2 show that DTBP is a competitor, along with the olefin **II**, for the iodide **I**. In a separate experiment, it was demonstrated that as the [DTBP] in the initial reaction mixture was increased, the yield of side products 1 and 2 increased accordingly. Side product 1 shown above, arises from the coupling of the radical $^\bullet CH_2C(=O)CH_3$ to the iodide **I**. It is reported [29] that proton abstraction by either $CH_3^\bullet$ or $(CH_3)_3CO^\bullet$ [27,30] is known to occur; indeed the authors observed the presence of *t*-butanol in the crude reaction mixture (spectrum not shown). It is therefore possible that the alkoxy radical $(CH_3)_3CO^\bullet$, arising from the homolytic cleavage of DTBP [11–13], or the methyl radical $CH_3^\bullet$ (although the presence of CH_4 was not detected) abstracts a proton from acetone as is known to occur [31,32]; the radical species thus generated either couples with the perfluoro radical $CF_3CF_2^\bullet$ or adds to the corresponding iodide **I**. The species $ICH_2C(=O)CH_3$ was not detected via NMR spectroscopy. Side product 2 is the outcome of the coupling of the alkoxy radical $(CH_3)_3CO^\bullet$ to the iodide **I** or to its corresponding radical species $CF_3CF_2^\bullet$.

Studies by Marchionni and Srinivasan [33] and by Paciorek and Kratzer [34] have demonstrated that ketone and ether terminals of the type shown in species 1 and 2 above are normally observed in peroxide-initiated polymerizations. Furthermore, both ketone and ether termini are stable at 140 °C under radical conditions and therefore can be detected and isolated in the crude reaction mixture at the end of the polymerization reaction. This is in further support of the side reaction products 1 and 2 observed.

A substantial presence of homocoupling of $CH_3^\bullet$ radicals leading to C_2H_6 was not observed in contrast to Cope et al. [25]. A probable explanation is that the concentration of $CH_3^\bullet$ at any point in time during the course of the coupling reaction was very low with respect to the iodide **I** and therefore was quickly quenched.

3. Conclusions

Peroxide-initiated radical coupling reactions of a perfluorinated alkyl iodide involve exclusively a Markovnikov mechanism yielding secondary iodides. The secondary iodides observed arise from both single and multiple coupling reactions. Radical coupling evolves side products due to the radical initiator employed, which adds mainly to the perfluoroiodide.

Applying this model study to a real polymeric system implies that one should expect, along with the cross-linked products, polymers with ether or ketone end-groups.

4. Experimental details

4.1. Reagents

Both C_2F_5I (**I**) and $C_8F_{17}I$ (**Ia**) were purchased from Aldrich and were used without further purification. Di-*t*-butyl peroxide was purchased from Carlo Erba and was used without further purification.

4.2. Analysis

^1H, ^{19}F, ^{13}C, and correlated NMR spectra were recorded on a Varian spectrometer operating at 400 MHz.

Gas chromatograms were recorded on a GC 8000Top Carlo Erba gas chromatographer employing a capillary 0.54 mm, 25 m long silicone-packed column.

Mass spectra were recorded on a Finnigan MAT SSQ700 chromatographer employing a methyl silicone CPSIL (Varian-Chrompack) column (50 m, i.d. = 0.32 mm; thickness = 5 m).

Boiling points of products **IV** and **V** were estimated employing a micro-distillation apparatus.

4.3. Synthesis 8-vinyl perfluoro-octane (*II*)

The synthesis of (**II**) is already reported in the literature [35–37]. We report here a slightly modified version.

Octyl perfluoro iodide, $C_8F_{17}I$ (50 g, 91.6 mmol), was placed in a 45 ml stainless steel autoclave equipped with a magnetic stirrer and a digital pressure gauge. The autoclave was mechanically sealed, evacuated and washed with N_2. The evacuated autoclave was placed in an oil bath and heated in order to reach an internal temperature of 160 °C.

Fifty atmospheres (35 mmol) of C_2H_4 were then loaded in the autoclave. As the reaction proceeded, ethylene was continuously added until no more ethylene was consumed. The total reaction time was 8 h. The autoclave was then cooled and the crude reaction product was analyzed by ${}^{19}F$ and ${}^{1}H$ NMR, FT-IR and found to be $CF_3(CF_2)_7CH_2CH_2I$ (**Ib**) 51.6 g. Conversion = 99%, yield = 98.2%. The crude product was used without further purification (1% starting iodide and 0.5% telomeric product identified as $CF_3(CF_2)_7(CH_2CH_2)_2I$ were also obtained). **Ib** (50 g, 87.1 mmol) was dissolved in 50 ml of anhydrous ethanol and stirred at 65 °C in a three necked round bottom flask. When the reaction mixture reached 65 °C, 1.2 eq. of ethanolic KOH were slowly added by means of a graduated dropping funnel. The reaction was moderately exothermic and care was needed not to exceed 75 °C. The crude reaction product was filtered to separate KI and the ethanol was distilled under reduced pressure; 35 g, 78.5 mmol, of the desired product **II** were obtained. Conversion = 99%, yield after distillation = 88.5%. The product was identified by ${}^{19}F$ and ${}^{1}H$ NMR spectroscopy and by FT-IR.

${}^{19}F$ NMR: −84 ppm (s, CF_3–), −117 ppm (s, 8–CF_2–), −124,8 ppm (s, 7–CF_2–), −125.2 ppm (s, 3,4–CF_2–), −126.1 ppm (s, 6–CF_2–), −127 ppm (s, 3–CF_2–), −130 ppm (s, 2–CF_2–).

${}^{1}H$ NMR ($CDCl_3$): 5.95 ppm (m, $-CH{=}C\underline{H_2}$), 5.9 ppm (m, $-C\underline{H}{=}CH_2$).

FT-IR (ν, cm^{-1}): 1651 ($-CH{=}CH_2$ st.), 1080–1200 (CF_3– and –CF_2– st.).

GC (70 °C for 1 min, slope to 210 °C at 15 °C/min, 210 °C for 4 min): $t_{ret} = 3.92$ min.

4.4. Model coupling reaction

I (2.03 g, 5.87 mmol), **II** (1.745 g, 3.9 mmol), DTBP (0.0427 g, 0.195 mmol, 0.05 eq.) and 2 ml of Galden® D-100 (perfluorobutyltetrahydrofuran 80% and perfluoropropyltetrahydropyran 20% with bp = 100 °C), were placed in a 10 ml two necked, round bottom glass ampoule equipped with a Teflon® "sure seal" stopcock and a magnetic stir bar. The ampoule was placed in a dry ice bath at −80 °C and the air inside removed by flushing with N_2 for 20 min. The ampoule was then sealed and placed in an oil bath at 140 °C and magnetically stirred for 3 h equivalent to four half lives of the DTBP. Due to the experimental conditions chosen, all of the reagents were in the liquid phase during the entire course of the reaction. The crude reaction product was then washed in H_2O. The organic layer was collected, dissolved in CH_2Cl_2 and dried over $MgSO_4$. The solvents were carefully distilled and the crude mixture analyzed by ${}^{1}H$, ${}^{19}F$ NMR and ${}^{13}C$ NMR. Conversion (based on the limiting reagent **II**) = 46% (mol%).

Two major coupling products **IV** and **V** and three minor side reaction products 1–3 were observed by NMR spectroscopy in the crude, washed reaction mixture. The calculated yields of the sum of the main coupled products **IV** and **V** and the sum of the three side products 1, 2 and 3 were, respectively, 42 ± 2 and 4 ± 0.2% (mol%). The selectivity of coupled products to side products was therefore approximately 9:1.

The crude reaction mixture was redistilled to eliminate the low boiling side products 1 (bp ≈ 70 °C), 2 (bp ≈ 80 °C) and 3 (bp = 41 °C), the solvent (Galden® D-100) and the residual starting compound **II** (bp = 135 °C). Starting compound **I** was eliminated during work-up since it has a bp = 13 °C. A viscous orange residue was obtained which was composed of 90% (mol%) of compounds **IV** and **V** and 10% (mol%) of residual starting material **II**.

The yield of the singly coupled product **IV**, was 25% and the yield of the multiply coupled product **V** was 16.7%, as determined by ${}^{1}H$ (Fig. 2) and ${}^{19}F$ (Fig. 4) NMR spectroscopy. The selectivity of the singly coupled product **IV** and of the multiply coupled product **V** is therefore, respectively, 60 and 40%.

NMR (**IV**): ${}^{1}CF_3{}^{2}CF_2{}^{a}CH_2{}^{b}CHI{}^{3}CF_2{}^{4}CF_2{}^{5}(CF_2)_4{}^{6}CF_2\,{}^{7}CF_3$.

${}^{19}F$: 1 (−86.2 ppm); 2 (−118 ppm, AB system); 3 (−99 and −110 ppm); 4 (−116.5 ppm AB system); 5 (−122 ppm); 6 (−126 ppm); 7 (−81.1 ppm).

${}^{1}H$: a (3.3 ppm); b (5 ppm).

${}^{13}C$: a (35 ppm); b (5.2 ppm); doublet of triplets, ${}^{1}J({}^{13}C, {}^{1}H) = 152$ Hz and ${}^{2}J({}^{13}C, {}^{19}F) = 26$ Hz.

bp (**IV**): 170–180 °C.

NMR (**V**): ${}^{1}CF_3{}^{2}CF_2{}^{c}CH_2{}^{d}CH[{}^{e}CH_2{}^{f}CHI{}^{3}CF_2{}^{4}CF_2{}^{5}(CF_2)_4{}^{6}CF_2{}^{7}CF_3]{}^{8}CF_2{}^{4}CF_2{}^{5}(CF_2)_4{}^{6}CF_2{}^{7}CF_3$.

${}^{19}F$: 1 (−85.8 ppm); 2 (−118 ppm AB system); 3 (−97 and −112 ppm); 4 (−116.5 ppm AB system); 5 (−122 ppm); 6 (−126 ppm); 7 (−81.1 ppm).

${}^{1}H$: c (2.7–2.8 ppm); d (3.4 ppm); e (2.4 ppm); f (4.89 ppm).

${}^{13}C$: c (29 ppm); d (37.3 ppm); e (32.8 ppm); f (22.5 ppm).

bp (**V**): >240 °C (dec.).

${}^{1}H$ NMR (side product 1—not isolated): –CH_3 (2.1 ppm, s; 3H); –$CH_2C({=}O)$– (3.3 ppm; broad t; 2H).

${}^{19}F$ NMR (side product 1—not isolated): –CF_3 (−86 ppm; shielded by **IV** in Fig. 2); –CF_2– (−118 ppm; shielded by **IV** in Fig. 2).

${}^{1}H$ NMR (side product 2—not isolated): –CH_3 (1.3 ppm; s; 9H).

${}^{19}F$ NMR (side product 2—not isolated): –CF_3 (−86 ppm; shielded by **IV** in Fig. 2); –CF_2O– (−80 ppm).

${}^{1}H$ NMR (side product 3—not isolated): –CH_3 (2.2; s; 3H).

Acknowledgements

We wish to thank Mrs. Elisa Restelli and Dr. Cristina Grossi for the NMR spectra, Dr. Patrizia Dardani for the GC–MS spectra and Prof. Luciana Giovannetti for a critical review of this work.

References

[1] I. Wlassics, V. Tortelli, W. Navarrini, M. Albano, US Patent 5,902,857 (1999); [CA 127 (1994) 6039].

[2] M. Albano, C. Pizzi, I. Wlassics, US Patent 5,948,868 (1999); [CA 126 (1999) 344397].

[3] D. Reyx, I. Campistron, C. Cailloud, Macromol. Chem. Phys. 196 (1995) 775.

[4] W.W. Schmiegel, Die Angew. Macromol. Chem. 76/77 (1979) 39.

[5] A. Logothetis, Prog. Pol. Sci. 14 (1989) 251.

[6] A. Apotheker, J. Finley, P. Krusic, A. Logothetis, Rubber Chem. Technol. 55 (1982) 1004.

[7] P. Krusic, J. Kochi, J. Am. Chem. Soc. 93 (1971) 846.

[8] P. Meakin, P. Krusic, J. Am. Chem. Soc. 95 (1973) 8185.

[9] B. Smart, P. Krusic, P. Meakin, R. Bingham, J. Am. Chem. Soc. 96 (1975) 7385.

[10] P. Krusic, R. Bingham, J. Am. Chem. Soc. 98 (1976) 230.

[11] G.R. McMillan, M.M. Wijnen, Can. J. Chem. 36 (1958) 1227.

[12] J.K. Allen, J.C. Bevington, Proc. R. Soc. A262 (1961) 271.

[13] F.F. Rust, F.H. Seubold, W.E. Vaughan, J. Am. Chem. Soc. 72 (1950) 228.

[14] D.S. Ashton, D.S. Shand, J.M. Tedder, J. Am. Chem. Soc., Perkin Trans II (1975) 320.

[15] P. Tarrant, J.P. Tandon, J. Org. Chem. 34 (1969) 864.

[16] F. Guida-Pietrasanta, A. Ratsimihety, G. Caporiccio, J. Fluorine Chem. 68 (1994) 71.

[17] R.N Hazeldine, M.J. Newlands, B.R Iles, Br. Patent 1075101 (1967); [CA 67 (1967) 100240].

[18] Y.K. Kim, A.G. Smith, O.R. Pierce, J. Org. Chem. 38 (1973) 1615.

[19] V. Arcella, G. Brinati, M. Albano, V. Tortelli, US Patent 5585449 (1996); [CA 123 (1996) 259509].

[20] J.M. Tedder, J.C. Walton, Acc. Chem. Res. 9 (1976) 183.

[21] (a) F. Jeanneaux, M. Le Blanc, A. Cambon, J. Cambon, J. Fluorine Chem. 4 (1974) 261;
(b) K.B. Wiberg, W.E. Pratt, W.F. Baily, J. Org. Chem. 45 (1980) 4936;
(c) C. Tonelli, F.C. Schilling, R.E. Cais, Macromolecules 14 (1981) 560.

[22] M. Apostolo, V. Arcella, G. Storti, M. Morbidelli, Macromolecules 35 (2002) 6154.

[23] V. Arcella, M. Apostolo, Rubber World (2001) 27.

[24] V. Arcella, M. Apostolo, Fluoropolymers 2000, Presentation 26, Savannah, GA, USA, 2000.

[25] J. Cope, A.C. Grieg, J.M. Tedder, J. Chem. Faraday Trans. 1 71 (1975) 592.

[26] C. Walling, Free Radicals in Solution, Wiley, New York, 1957 (Chapter 3).

[27] J.P. Sloan, J.M. Tedder, J.C. Walton, J. Chem. Soc., Perkin Trans II (1975) 1846.

[28] J.M. Tedder, J.C. Walton, L.L.T. Vertommen, J. Chem. Soc., Perkin Trans II (1978) 1040.

[29] M. Newcomb, R.M. Sanchez, J. Kaplan, J. Am. Chem. Soc. 109 (1987) 1195.

[30] H.Q. Xie, W.E. Baker, in: T.C. Chung (Ed.), New Advances in Polyolefins, Plenum Press, New York, 1993, pp. 109–110.

[31] A.I.I. Taha, R.R. Kuntz, J. Phys. Chem. 73 (1969) 4406.

[32] H. Arica, N.L. Arthur, Aust. J. Chem. 36 (1983) 2185.

[33] G. Marchionni, P. Srinivasan, Fluoropolymers 1992, Paper 14, UMIST—Manchester, GB, 1992.

[34] K.J.L. Paciorek, R.H. Kratzer, J. Fluorine Chem. 67 (1994) 169.

[35] B. Ameduri, B. Boutevin, M. Nouiri, M. Talbi, J. Fluorine Chem. 74 (1995) 191.

[36] Z. Szlavik, G. Tarkanyi, A. Gömöry, J. Rabai, Org. Lett. 2 (2000) 2347.

[37] S. Kohjiya, M. Kozuyuki, S. Yamashita, Y. Shibata, J. Mater. Sci. 25 (1990) 3368.